RADIO OBSERVATIONAL CONSTRAINTS ON PULSAR EMISSION MECHANISMS

J.M. Cordes
Astronomy Department and NAIC, Cornell University

...vibrating like the simplest/living crystal/and making spirit loops/ of exquisite complexity and power. (M. McClure, Jaguar Skies)

ABSTRACT

A discussion is made of those observations that place constraints on the pulsar emission mechanism and its location in the pulsar magnetosphere. After reviewing the salient features of pulsar radiation, a number of issues are confronted, including (1) whether coherence is broadband or narrowband and, accordingly, (2) whether the emission frequency is mapped into radius and/or magnetic polar angle; and (3) whether pulse structure (micropulses and subpulses) represents angular or temporal structure. It is proposed that pulse nulling, mode changing, and quantized drift rates for subpulses are related to discrete states of the particle flow in polar cap models.

1. INTRODUCTION

The present is an exciting time for the study of the pulsar radio-emission mechanism. Theory has progressed to the point where observations, rather than surveying diverse phenomena, now test specific details of magnetospheric models, particle acceleration mechanisms, and coherence mechanisms. This can be contrasted with the only previous meeting that has specifically confronted the emission mechanism, the Stanford Symposium of 1974 (Manchester 1974), at which a large gap between observation and theory was evident. The "critical experiments" proposed at that meeting were largely empirically motivated and did not in general test specific magnetosphere/emission-mechanism models. What seemed like an overwhelming variety of apparently disconnected phenomena led T. Gold to ask, "Can any observational facts be discarded?" At that time no one knew the answer to that question although the mood called for an affirmative answer.

In the intervening time, no really new phenomena have been discov-

W. Sieber and R. Wielebinski (eds.), Pulsars, 115–131.

ered. Rather, the known ones have been explored in tremendous detail, to the point where some phenomena appear to be related (e.g. the connection between drifting subpulses and pulse nulling found by Unwin et al. 1977; see below) and they in fact impinge on specific features of theory. One such theory had its seeds in the Stanford Symposium and Sturrock's (1971) seminal theory: the spark-gap model of Ruderman and Sutherland (1975) in which pair production discharges at the magnetic polar cap control subpulse drift and the replenishment of charges in the open field portion of the magnetosphere. This model has evolved considerably in the last 5 years, receiving more detailed treatment of particle injection at the neutron star surface, propagation effects in the magnetosphere, and studies of coherence mechanisms. To this author, the pulsar situation may be contrasted with the study of radio galaxies and quasi-stellar objects: In the latter case, the emission mechanism (incoherent synchro-compton radiation) is well understood but the energetics and geometry of particle beams are not. For pulsars, the energetics (of radio emission) and geometry appear to be relatively well-fathomed (in polar cap models) compared to the emission mechanism, about which we do not know how coherence is established, whether it is broadband, how circular polarization is produced, etc.

In this paper my aim is to discuss observational constraints on the magnetosphere and emission mechanism, starting on a general basis and proceeding to a treatment of detailed points-of-contact between polar cap models and observation. Observationally the focus will be on fluctuations in the total intensity; polarization will be mentioned only briefly because it is dealt with by Backer in these proceedings.

2. COHERENT RADIATION FROM PULSARS AND POLAR CAP MODELS

2.1 Basic Phenomena

Figure 1 shows a single pulse from PSR 0950+08. Structure from 0.1 to 5 ms is evident with maximum flux densities $\sim 10^3$Jy, corresponding to a brightness temperature $\sim 10^{27}$K, which indicates a coherent radiation mechanism. The average of 300 pulses in the figure is a waveform (or average profile) that is stable over the last 12 years, requiring that radiation be produced where the magnetic field is energetically dominant over the radiating plasma. If the waveform is considered to measure pulsar climate and a single pulse the weather, then pulsar climate is considerably more stable than the Earth's which shows ice ages, etc., on 10^4 - 10^5 yr. time scales, because observations over the last decade represent $10^{8.7}$ pulsar years.

Short-duration ($\sim$ 0.1 ms) spikes in figure 1 are micropulses while broader structure comprises subpulses. They are distinct constituents because the autocorrelation function of the intensity (computed over a single pulse and averaged over many pulses) typically shows separate micropulse and subpulse features (Hankins and Rickett 1975; Cordes 1979b).

https://doi.org/10.1017/S0074180900092767 Published online by Cambridge University Press

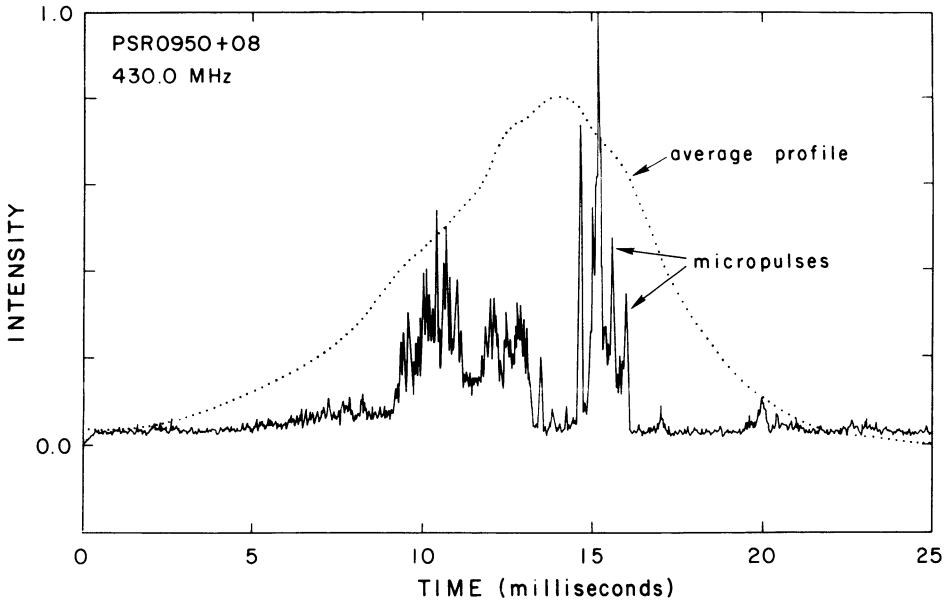

Figure 1. A single pulse and average profile of 300 pulses obtained at the Arecibo Observatory.

Recently, Ferguson (1981) has suggested that micropulses and subpulses are produced in independent emission regions. While this may or may not be true, there is no compelling evidence supporting this assertion. For pulsars that display distinct subpulses, the micropulses almost always appear as internal structure rather than occurring (e.g.) in between subpulses.

Micropulses have been observed in $\sim$ 12 pulsars with widths ranging from 1 μs to 4 ms and being roughly proportional (with large scatter) to period (Cordes 1979b). Micropulses are often quasi-periodic with quasi-periods (P_μ) ranging from 0.1 to 5 ms (Cordes 1976a; Boriakoff 1976; Ferguson and Seiradakis 1978; Bartel et al. 1980; Cordes et al. 1980). The quasi-periodicity is a low-Q process: individual subpulses rarely contain as many as 10 micropulses and the period can change within micropulse sequences as well as from subpulse to subpulse. Out of $\sim$ 10 pulsars investigated, the 3 that show the most consistently occurring quasi-periodic microstructure (0809+74, 1944+17, and 2016+28) also display drifting subpulses, whose appearance is correlated with small period derivatives (Huguenin et al. 1970b).

Drifting subpulses refer to subpulses that appear progressively earlier (sometimes later) in successive rotation periods. Intensity contours appear as bands with a characteristic spacing at a fixed pulse longitude, P_3. Often there will be two subpulses in a single rotation period, implying a separation of bands, P_2. For some pulsars both P_2 and P_3 are constant, or nearly so (e.g. PSR 0809+74) while

https://doi.org/10.1017/S0074180900092767 Published online by Cambridge University Press

others show statistical variations of P_2 and/or P_3; finally, two pulsars (0031-07 and 1919+21) show quantized values of P_3, suggesting that the magnetosphere enjoys several metastable states (Huguenin et al. 1970a; Backer 1973).

Mode change refers to the average waveform alternating between two preferred shapes on time scales of order several hundred rotation periods. Generally, the mode change conserves the number and position of components, but alters their relative amplitudes.

Nulling is the occurrence of rotation periods with no detectable emission. Episodes of nulling last for one to several hundred or more periods, some pulsars being in the off state more than the on state. Like subpulse drifting, nulling tends to occur in pulsars with smaller values of period derivative and hence, presumably, smaller magnetic fields (Huguenin et al. 1970b; Ritchings 1976). Unwin et al. (1977) discovered the remarkable happenstance in PSR 0809+74 that the last drifting subpulse before a null and the first one after the null have the same pulse longitude. That is, subpulse drifting ceases during a null.

Table 1

EVIDENCE FAVORING POLAR-CAP-HOLLOW-CONE BEAM MODELS

OBSERVABLE	PROPERTY
Waveform Shape	1. Mirror symmetry of lobe structure. 2. Relative number with 1 lobe, multiple lobes, interpulses. 3. Stable over 10 yr.; implies radiation from magnetic-field-dominated flow. 4. Dispersion fiducial point $\approx$ profile midpoint $\Longleftrightarrow$ magnetic pole.
Waveform Width	$\Delta\Theta \propto \nu^{-\alpha}$, $0.0 \lesssim \alpha \lesssim 0.6$ radius to frequency mapping and flaring of open-field-line region.
Pulse-to-Pulse Fluctuations	Mirror symmetry about fiducial point.
Polarization Angle Sweep	S-shaped signature over $\approx 180°$ for multiple-lobed waveforms. Linear sweep $< 180°$ for single-lobed waveforms.

https://doi.org/10.1017/S0074180900092767 Published online by Cambridge University Press

2.2 Hollow-Cone Beams

Evidence can be marshalled which identifies the average waveform with a rotating hollow-cone beam that coincides with the magnetic polar region(s) of the magnetosphere. As summarized in Table 1 this evidence includes the stability and approximate symmetry of average waveforms and the relative number of waveforms with one lobe, two or more lobes, and interpulses. The probability of seeing one lobe is related to the associated probability of the line of sight making the appropriate 'impact parameter' with the beam. Consequently, the distribution of waveform types and widths can be predicted from distributions for $\underset{\sim}{\Omega} \cdot \underset{\sim}{m}$ and $\underset{\sim}{\Omega} \cdot \hat{n}$ where $\underset{\sim}{\Omega}$=rotation axis, $\underset{\sim}{m}$=magnetic moment, and $\hat{n}$=line of sight. The results assuming uniform distributions for the latitudes of $\underset{\sim}{m}$ and $\hat{n}$ are consistent with the observed occurrences (Backer 1976; Proszynski 1979), although it is clear that the angular beam size is not the same for all pulsars. Moreover, some pulsars show 3 or 5 components, suggesting the beam has a central component or, in some cases, two concentric annular beams. Such augmented features to the hollow-cone beam are purely ad hoc and are not understood in magnetospheric models. Finally, interpulses (components at large [$\gtrsim 150°$] longitude separations from 'main' pulse components) are consistent with their arising from an opposite magnetic pole and hence $\underset{\sim}{\Omega} \cdot \underset{\sim}{m} \approx 0$. This interpretation is contentious, however. Interpulse/main pulse emission alternatively may signify a large cone angle for a single beam or a different kind of emission altogether (Manchester and Lyne 1977), ideas to which we will devote more attention later.

2.3 Polar Cap Models

Physically, the hollow-cone beam and many of its properties are nicely accounted for in polar cap models (see Ruderman 1980 for a recent review), where relativistic particle flow occurs along field lines connecting the magnetic polar cap to the world external to the velocity of light cylinder. Acceleration occurs by virtue of rotation-induced electric fields and the fact that not all field lines close inside the light cylinder. Hollow-cone radiation beams arise in two ways: particle flow may itself show hollow-cone structure owing to boundary conditions (Arons 1979) or the radiation produced by the flow may depend inversely on field-line curvature which goes to infinity at a magnetic pole.

The details of the polar cap model are given as a flow diagram in figure 2, where magnetospheric currents are shown to give rise to both coherent radiation and to the spindown of the star. Recent work (Cheng and Ruderman 1980; Arons and Scharlemann 1979; Michel 1979; Kennel et al. 1979) has focused on the particle content of the flow that emanates from the polar cap. The kinds of flow include (1) charge separated flow: ions and positrons in some regions, electrons in others; (2) charge neutral flow composed of electrons and positrons. Sources of particles (e.g. space-charge-limited thermionic emission, X-ray annihilation in 10^{12} G fields; pair production in ions' Coulomb fields) may

https://doi.org/10.1017/S0074180900092767 Published online by Cambridge University Press

differ between pulsars with different periods, surface temperatures, and magnetic fields and certain intensity variations may be a direct consequence of competition between these sources of particles (Cheng and Ruderman 1980)

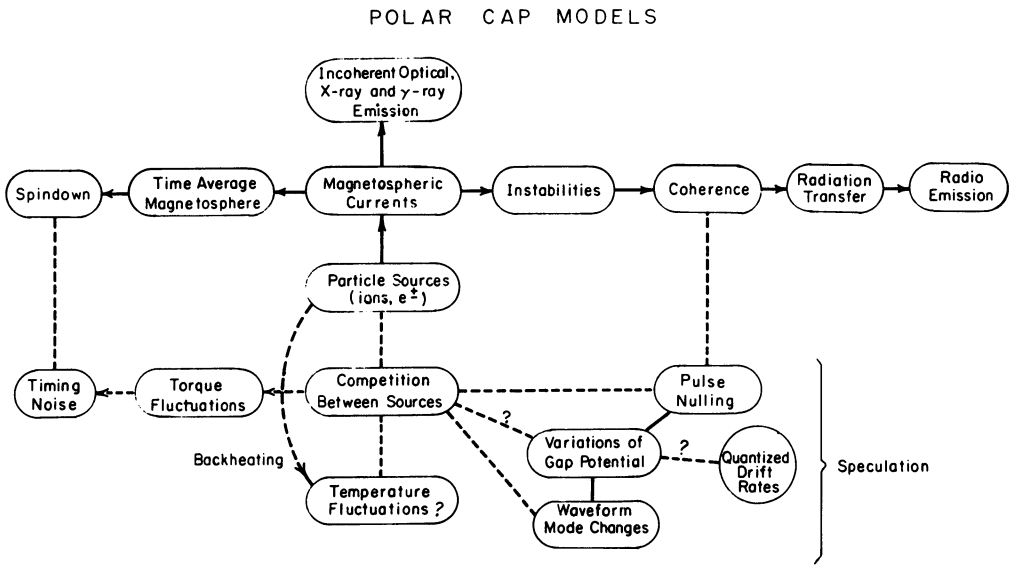

Figure 2. Flow chart for polar cap models. Solid lines connect orthodox features of polar cap models. Dashed lines are speculative.

2.4 Observed and Predicted Time Scales

Intensity variations occur on time scales from nanoseconds to millions of years, the former deduced from the reciprocal radiation frequency, the latter from the absence of pulsars with $P > 5$ s combined with knowledge of their spindown rates. Observed or inferred time scales are shown in figure 3 along with those associated with neutron stars in general and polar cap models in particular. Observational and theoretical time scales show considerable congruence but a cynic might view this as pure numerology. Arons (1979) has pointed out that particle flow shows no variations slower than the gap-discharge time ($\sim$10μs) if such variations are electrodynamically produced. However, Cheng and Ruderman (1980) point out that competition between particle sources brings other time scales into play, such as heating and cooling times for the polar cap. Some such competition may be required to produce temporal fluctuations in the flow on time scales larger than 10μs. Another relevant time scale ($\sim P$) is that for beam wavering which may occur because induced currents modify the magnetic field structure (Arons 1980). Both temperature fluctuations and beam wavering would also cause torque fluctuations and these may be manifested as pulsar timing noise (Helfand et al. 1980; Cordes and Helfand 1980; Cordes and

https://doi.org/10.1017/S0074180900092767 Published online by Cambridge University Press

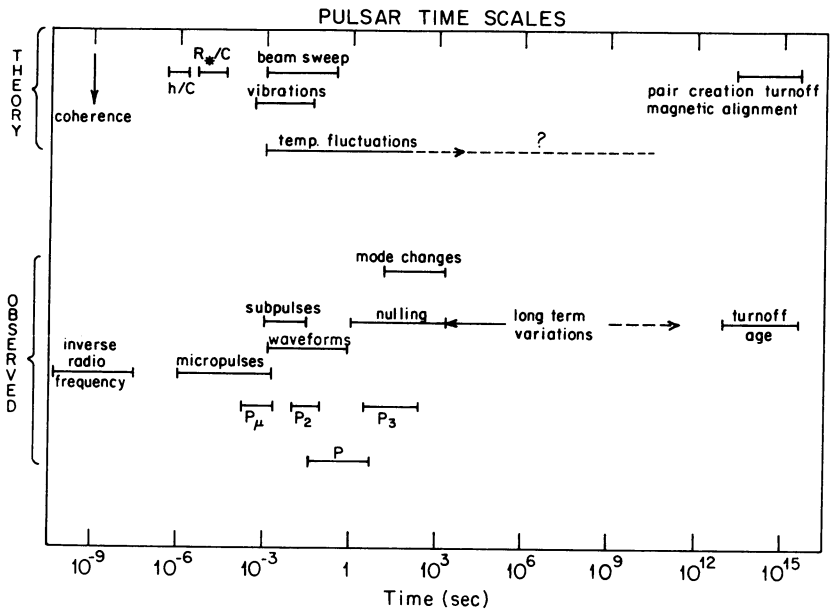

Figure 3.

Greenstein 1981), as is shown in figure 2.

2.5 Coherence

Radio pulsars are observable only because their radiation is coherent, but coherence is manifest in at most 3 ways: (i) brightness temperatures of order 10^{25} to 10^{31} K; (ii) average radio spectra of a 'low pass' form with frequency cutoffs between 1-10 GHz; and possibly (iii) large fluctuations in intensity on a variety of time scales.

Average spectra are typically piece-wise powerlaws $\propto \nu^{-\alpha}$ with α often larger at higher frequencies. Some pulsars show low-frequency turnovers below 200 MHz that are absent in others which have a single value of α from 40 MHz to 10 GHz (Sieber 1973; Bruk et al. 1978). The falloff with increasing ν has commonly been interpreted as a length scale $\sim$1-10 cm associated with coherence. Taken literally, charge bunches of this size could produce the observed spectra, but it is difficult to conceive of mechanisms for producing such bunches that do not involve plasma instabilities and, hence, maser effects. Observations may never distinguish between 'pure' maser action and pure bunching ('antenna') coherence. Of greater importance is whether coherence is locally or instantaneously broadband or narrowband. Observations discussed below suggest that some emission components may be narrowband, others broadband.

https://doi.org/10.1017/S0074180900092767 Published online by Cambridge University Press

The intensity can change by a factor of 100 or more on time scales of tens of microseconds (Hankins 1971, 1972; unpublished data). Coherence implies that N particles yield an intensity (I_N) that is greater than the sum of their individual intensities (I_1): $N I_1 \leq I_N \leq N^2 I_1$. Consequently small changes in number of particles radiating coherently can produce large changes in intensity such as those observed. It is by no means certain, however, that intensity and coherence fluctuations are linked, as is assumed in comparing the Crab pulsar's possibly incoherent--and steady--optical emission with coherent radio emission.

2.6 Incoherence

While coherence is clearly required and some intensity variations may indeed signify coherence fluctuations, observations indicate that micropulses and subpulses are incoherent ensembles of coherent emissions. The most accurate picture is that coherence fluctuations occur on time scales of order the reciprocal spectral bandwidth ($\sim$1 ns) and all 'macroscopic' intensity variations such as micropulses are incoherent sums of large numbers of nanopulses. That is, a micropulse is an example of a 'sophisticated' signal: one that has a time-bandwidth product $>>1$. This picture has been tested by calculating the intensity autocorrelation function whose features include (i) a spike at zero lag of width $\sim 1/\Delta\nu$ where $\Delta\nu$ is the receiver bandwidth and (ii) broader features corresponding to micropulses and subpulses. The amplitude of the zero lag spike depends on the statistics of fluctuations that occur on $\Delta\nu^{-1}$ time scales. Computations (Rickett 1975; Cordes 1976a,b; Hankins and Boriakoff 1978) indicate that such fluctuations have Gaussian statistics. One can infer using the Central Limit Theorem that in an interval of $\sim$1μs, the pulsar signal receives contributions from a large number of independent coherent emitters. This number may be larger than $N \sim 1\mu s/1ns = 10^3$.

Consequently, pulse features (e.g. micropulses and subpulses) do not reflect single coherent emitters. Micro/subpulse time scales refer to length scales of 'clouds' of coherent emitters.

2.7 Radiation Efficiency

The radio luminosity L, calculated as $L = S_{400} D^2 \Delta\nu$ (S_{400} = 400 MHz flux density, D = distance, $\Delta\nu \approx 1$ GHz is the typical bandwidth of a pulsar spectrum) represents a negligible fraction of the rotational energy loss $\dot{E}=I\Omega\dot{\Omega}$. The ratio $L/\dot{E}$ ranges between $10^{-9.5}$ for the Crab pulsar and 10^{-2} for PSR 1819-22. However, it is well known from magnetosphere models (e.g. Michel 1969) that rotational energy in the near wave field ($r \lesssim r_{LC} = c/\Omega$) is carried away mostly by fields than by particles. Consequently, it is more illuminating to compare L with the energy loss rate in particles, $\dot{E}_p$. Estimates of $\dot{E}_p$ vary between models (see Ruderman 1980 and Arons 1979 for reviews), but

$$\dot{E}_p \gtrsim 10^{30} (B_s/10^{12} \text{ G}) P^{-2} \text{erg s}^{-1}, \quad (1)$$

https://doi.org/10.1017/S0074180900092767 Published online by Cambridge University Press

where the coefficient is accurate to order of magnitude, the exponents of B_s and P are approximate, and B_s is the surface magnetic field. Constructing $L/\dot{E}_p$, we find a range between 10^{-5} and 1 if we derive B_s from P and $\dot{P}$ according to

$$B_s = (I\ c^3\ P\ \dot{P})^{1/2} / 2\pi R^3 \qquad (2)$$

which is applicable for a dipolar magnetic field (Gunn and Ostriker 1970; Goldreich and Julian 1969). Thus it is clear in some cases that the radiation mechanism is highly efficient and that radiation reaction may be important for the particle flow.

A number of additional conclusions can be made by looking at the statistics of L and other pulsar parameters. First, L is virtually uncorrelated with $\dot{E}$. Indeed the Crab and Vela pulsars, which have the two largest values of $\dot{E}$, have unextraordinary radio luminosities. This suggests that the emission mechanism 'works' in only a small volume of the appropriate parameter space and therefore, for pulsars with different abilities in accelerating and creating particles, the right conditions (especially particle density) will be found at different altitudes in the open-field line region for different pulsars. Hence we should expect a variation of beam width, which depends on radius (as $r^{1/2}$ for dipolar fields), with rotation period.

2.8 Radiation Energy Densities

The energy density of the radiation field at the Earth $u_{rad} = S\Delta\nu/c$ is larger by a factor $(D/r)^2$ at the pulsar, where S = flux density, $\Delta\nu$ = radiation bandwidth, D = pulsar - Earth distance, and r = distance of emission region from the neutron star. For strong micropulses from PSR 1133+16 ($S \gtrsim 10^3$Jy, $\Delta\nu \gtrsim 0.2$ GHz) we have $u_{rad} \sim 1$ erg cm^{-3} at $r = r_{LC} = c/\Omega$ = light cylinder radius. At smaller radii, the energy density may not vary as an inverse square law if radiation and particles are not decoupled. Observational limits (§3.2) suggest, however, that decoupling radii are less than a few per cent of the light cylinder radius, so $u_{rad} \gtrsim 10^4$erg cm^{-3}. A direct comparison with particle or magnetic energy densities must account for relativistic motion towards the observer, which reduces the energy density in the particles' frame by a factor of γ^{-2} where γ is the Lorentz factor. If relativistic motion is due to corotation, as in light cylinder models, then $r/r_{LC} < 0.2$ or $r/r_{LC} > 0.98$ if the radiation energy density is to be smaller than that of the ambient magnetic field (u_B) (Manchester and Taylor 1977 p. 217; Bartel 1978). Magnetospheric models may rule out corotation at $r/r_{LC} > 0.98$. In polar cap models, $u_{rad} < u_B$ at radii that are consistent with observational limits.

2.9 Polarization Fluctuations: Geometric Rotation and Orthogonal Modes

As previously alluded to (Table 1), polarization waveforms (averages of the Stokes parameters over many pulses) are consistent with the polar-cap model as long as one takes into account orthogonal modes whose

relative strength varies with longitude so as to complexify an otherwise smooth position-angle (PA) rotation (Backer et al. 1976; Cordes et al. 1978; Backer and Rankin 1980). If one assumes that the PA of one of the modes reflects the direction of the ambient magnetic field (as projected on the plane of the sky), that the ambient field is dipolar, and that relativistic beaming causes the line of sight to sample essentially only one direction in pulsar coordinates, then the position angle rotation exhibits a signature and amplitude that depend primarily on the minimum angle (an 'impact parameter') that the line of sight makes with the magnetic pole. The signature is essentially geometric in nature. The observed signatures and amplitudes should be correlated with waveform shape (double-lobes show S-shaped curves, single lobes show linear curves $< 180°$), as is qualitatively true (Jones 1979), although there are exceptions which may be explained away as unusually hollow beams or non-dipolar field topologies.

The orthogonal mode phenomenon is ubiquitous and is manifested as transitions between orthogonal position angles that take place on micropulse (Cordes and Hankins 1977) and subpulse (Manchester et al. 1975) time scales. When the position angle jumps or rotates over 90°, the circular polarization often changes from left-hand to right-hand or vice versa (Cordes et al. 1978). That is, the orthogonal modes represent two orthogonal states of elliptical polarization.

Numerous explanations have arisen for the appearance of orthogonal polarization modes, including (1) changes in optical depth of two modes associated with the relevant medium, such as the optical depth of cyclotron scattering at high altitudes (Blandford and Scharlemann 1976); (2) birefringence in an electron positron plasma (Melrose 1979); (3) the presence of two emission components whose polarization is mutually orthogonal (Cheng and Ruderman 1979); and (4) polarization-dependent interaction of the wave field with a velocity-sheared and turbulent medium (Harding and Tademaru 1981).

Empirically, the PA indeed seems to be tied to the ambient magnetic field while the orthogonal mode transitions, which occur in part stochastically in single pulses and systematically as a function of longitude, are superposed. Consequently, it appears that pulsars are kind in allowing us to separate the geometric PA rotation with longitude from the actual occurrence of the two modes.

Mode transitions occur preferentially on micropulse and subpulse boundaries, implying that the turning on and off of the intensity (coherence?) is connected with two radiation modes or that a post-emission propagation effect is intensity dependent.

Before the identification of the orthogonal mode phenomenon, the 'fast' polarization transitions on subpulse time scales were taken as evidence that relativistic compression due to relativistic co-rotation velocities (i.e. light cylinder model) is occurring (e.g. Ferguson 1976). It seems now, however, that the mode transitions are a radiative

transfer effect and therefore the need for invoking relativistic corotation is obviated.

3. ANGULAR BEAMS AND TEMPORAL FLASHES

It has long been clear that observed temporal phenomena may reflect either angular beams rotating through the line of sight or temporal undulations that a corotating observer would also detect. We have already presented (§2.2, 2.3, Table 1) the support for an angular beaming interpretation of the waveform. Presently we demonstrate that smaller-scale beams cause subpulses whereas micropulses are evidently true temporal modulations. To do so we must first consider the frequency dependence of pulse structure and the radius-to-frequency mapping.

3.1 Average Waveform Frequency Dependence and the Radius-to-Frequency Mapping

Average waveforms change with radio frequency in two ways: through a weak variation of component separations or waveform width and/or through different components having different spectra. The latter variation has received little attention because the physics of the spectra is poorly understood. Component separations at low frequencies ($\lesssim$500 MHz) vary as $\Delta\Theta \sim \nu^{-\alpha}$ with $0.1 \lesssim \alpha \lesssim 0.5$ and $\langle\alpha\rangle = 0.26$ for 12 pulsars (Manchester and Taylor 1977); at higher frequencies α becomes smaller, typically zero, although some pulsars have $\alpha<0$. Counterexamples exist but, as argued below, these may arise because of the presence of more than one emission component.

Komesaroff (1970) first demonstrated that the $\nu^{-0.25}$ dependence (we adopt α=0.25 as the prototypical exponent) could be explained in the polar cap model if emission at a given radius is in a range of frequencies considerably smaller than the observed spectral width. Such a radius-to-frequency mapping (Cordes 1978) is inherent in any polar-cap model in which coherence is established via an instability whose largest growth rates are centered on the Doppler-shifted plasma frequency (e.g. Cheng and Ruderman 1977), which changes with radius. Though compelling, the observational support for such a mapping is primarily the $\nu^{-0.25}$ variation of the waveform. One must ask why, above a frequency ν_c, the dependence becomes weaker. An obvious possibility is that all frequencies above ν_c are radiated from the same radius. Another is that the field is non-dipolar near the surface of the star where higher-order multiples may be important. Thirdly, there is evidence (see below) that high-frequency ($\nu \geq \nu_c$) emission is dominated by a second emission component that, by implication, must not participate in the radius-to-frequency mapping. Finally, there is the intriguing possibility that the waveform ceases contracting at high-frequencies because of gravitational bending of ray paths. If one assumes a dipolar field, then ray paths that are initially tangent to the field lines are bent away from the radial direction by an amount

https://doi.org/10.1017/S0074180900092767 Published online by Cambridge University Press

$\delta\Theta \sim \Delta\Theta\ (R_s/r) \sim 1°$ where R_s is the Schwarzschild radius.

3.2 Retardation/Aberration Limits on Emission Radii

If we assume a radius-to-frequency mapping and a dipolar magnetic field, then the ratio of waveform widths at two frequencies yields the ratio of the corresponding emission radii. Absolute limits on the radii can also be gotten because differential aberration and retardation cause time delays that are separable from those due to cold-plasma dispersion in the interstellar medium (Cordes 1978 and Matese and Whitmire 1980). Upper limits on such delays imply maximum radii of order a few per cent of the light cylinder radius and minimum radii (corresponding to the highest frequencies) equal to a few to ten stellar radii.

Such limits suggest (Ruderman 1980; Cheng and Ruderman 1980) that particle number densities (and consequently emission radii) are smaller than those predicted by Ruderman and Sutherland (1975) owing to pair production being less efficient than previously thought.

3.3 Subpulse and Micropulse Spectral Dependences

Individual subpulses and micropulses have bandwidths of at least $\sim$200 MHz but they are certainly not as broadband as the entire pulsar signal. Subpulses are at least 70% correlated over 100 MHz separations for 10 pulsars (Taylor et al. 1975; Cordes and Rickett, in preparation) and 75% correlated from 327 MHz to 2.7 GHz for PSR 0329+54 and PSR 1133+16 (Bartel and Sieber 1978). Between 102 MHz and 1.7 GHz, however, subpulses from four pulsars are more weakly correlated (Bartel et al. 1980). Micropulses are prominent at low frequencies ($\lesssim$500 MHz) but are either infrequent or dominated by other emissions at high frequencies. The micropulse strength (measured as the fractional micropulse contribution to the variance) decreases with frequency for 4 pulsars: 1919+21, 1944+17, 2016+28, and 0809+74 (Cordes et al. 1980; Bartel et al. 1980). Individual micropulses are highly correlated for 0950+08 between 111 and 318 MHz (Rickett et al. 1975) and 1133+16 between 196 and 318 MHz (Boriakoff 1980). Ferguson and Boriakoff (1980) have found that micropulses are correlated between 430 and 1400 for 0950+08 but are uncorrelated for 1133+16 over the same range. Micropulses from 0809+74 at 102.5 MHz do not appear at 1720 MHz (Bartel et al. 1980).

The most revealing clues, however, concern the ν-dependence of the widths and separations of micropulses and subpulses. The drifting subpulses from 0809+74 (Bartel et al. 1980) and 0031-07 (Taylor et al. 1975) show $P_2 \propto \nu^{-0.25}$. Pulsars with double-component waveforms have subpulses occurring most frequently at component maxima (Craft 1970), so it can be inferred that subpulse separations generally partake of the $\nu^{-0.25}$ dependence. This is confirmed by direct comparison of subpulses at two frequencies for 1133+16 (Boriakoff 1980). Micropulses do not appear to have frequency-dependent separations. PSR 0950+08 has a waveform component-separation index $\alpha_w \approx 0.68$ between 40 and 400

MHz (Hankins and Cordes 1980) whereas micropulse separations ($P_\mu \propto \nu^{-\alpha_\mu}$) are constant between 111 and 318 MHz to the extent that $\alpha_\mu < 0.01$ (Rickett and Cordes 1981). Boriakoff (1980) has found a similar disparity between the waveform (α_w) and micropulse (α_μ) indices between 196 and 318 MHz for PSR 1133+16. Taken together, these results imply that micropulses are not simply smaller-width subpulses.

3.4 Subpulses as Angular Beams; Micropulses as Temporal Flashes

The discussion in the previous section suggests that subpulses are due to angular beams of size $\sim 4°$ (with large scatter; Taylor et al. 1975). Corroborating evidence lies in the polarization position-angle rotation across subpulses. Apart from orthogonal mode transitions (§2.9) on subpulse periphery, the PA rotates through subpulses of 1133+16 just as it does in the waveform. That is, the subpulse PA rotation is of a geometric nature as expected from an angular beam. Correlation functions of the Stokes parameters suggest that the PA does not rotate geometrically in micropulses from 2016+28 (Cordes 1979a) but this result is not definitive.

The picture we are left with is that subpulses are related to a columnar beam, perhaps a plasma stream confined to a tube of field lines, in which the radiated frequency is to some extent mapped into radius. Benford (1977) associates micropulses with similar filamentary

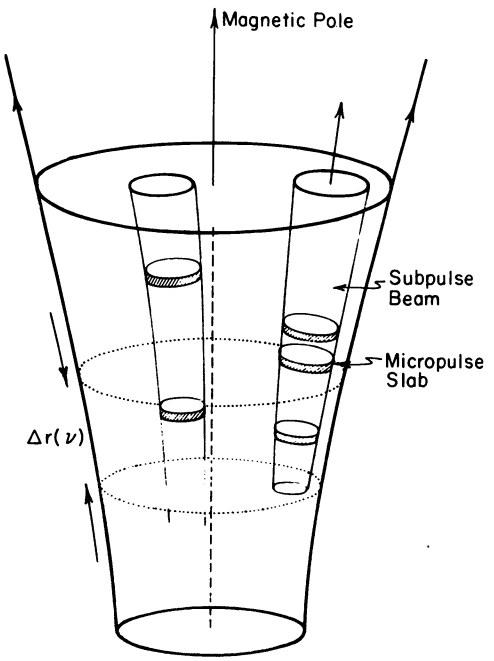

Figure 4.

Proposed model in which subpulses are due to beams that are radially modulated to give micropulses. Plasma flow is relativistic and emission at a given frequency arises in a small radial range, $\Delta r(\nu)$.

https://doi.org/10.1017/S0074180900092767 Published online by Cambridge University Press

beams, but that model is ruled out if the radius-to-frequency mapping holds on micropulse time scales. Consequently we are left with the situation in figure 4 where micropulses are due to slabs or pancakes (radial structure) in the subpulse beam (Rickett and Cordes 1981).

Physically, a number of things may be happening. Subpulse columns are necessarily related to the lateral extent of plasma injection near the stellar surface. Micropulse slabs may be produced by the plasma source (e.g. by stellar vibrations or oscillations in pair-producing discharges) or they may represent coherence fluctuations. Observations do not resolve whether micropulses partake in the radius-to-frequency mapping. If they do then a possible scenario is that (1) a plasma slab produces narrowband radiation at a frequency $\nu(r)$ as it propagates outward. (2) If the slab has radial extent Δr and angular extent $\Delta\Theta$ ($\Delta\Theta$ = subpulse beam width) and if the slab radiates at a given frequency for a time $\gtrsim \Delta r/c$, then the micropulse duration is equal to the larger of $\Delta r/c$ and $\Delta\Theta(1-\beta)/\Omega$ where Ω = rotation frequency. For reasonable parameters, the second time scale is less than 1μs. Micropulses produced at two frequencies (corresponding to two radii r_1 and r_2) arrive at the Earth virtually simultaneously: the arrival time difference is $\delta t \gtrsim (1-\beta)(r_2-r_1)/c \lesssim 0.1\mu s$ for $\gamma = 10^3$ and $r_2-r_1 \leq r_{LC}$. However, micropulses may not partake of the radius-to-frequency mapping if all frequencies are produced in a 'flash' at some radius. Such an occurrence is also consistent with observation.

Stinebring and Cordes (1981) have applied a skewness analysis to determine if micropulses are time symmetric or not. Asymmetries might be expected if the micropulses represent the establishment of coherence at a given ν by an instability followed by a radiative dissipation of the coherence: the respective rise and fall times may differ. Results on two pulsars (0950+08 and 2016+28) show no asymmetries.

3.5 Evidence for Two Emission Processes

Observations indicate that there are high and low-frequency regimes in which the character of the emission is markedly different. These include (1) a break frequency in the waveform-width vs. ν curve (Sieber et al. 1975); (2) a related breakpoint in the modulation index vs. ν curves for some pulsars (larger modulation of the intensity above the break frequency; Bartel et al. 1980); (3) the dominance of drifting subpulses and micropulses by featureless and less-modulated emission at high frequencies for some pulsars; and (4) the appearance of emission that is highly polarized but does not appear in orthogonal modes; rather, its PA is highly variable from pulse to pulse so as to depolarize averages of many pulses (Manchester et al. 1975; Cordes 1979b). The demarcation frequency between regimes varies between 0.2 and 1 GHz.

4. SUMMARY

Pulsar phenomena were surveyed while trying to understand them

within polar cap models. Subpulses and micropulses appear to represent angular and temporal plasma structure, respectively. Discrete states of the intensity (mode changes, nulling, quantized drift rates) may, along with micropulse quasi-periodicities, originate from competition between particle sources. Such competition may also be related to pulsar timing noise. Further work, both theoretical and observational, is needed to clarify these hypotheses.

I thank J. Arons, V. Boriakoff, A. Cheng, G. Greenstein, T. Hankins, J. Rankin, B. Rickett and J. Weisberg for helpful discussions. Thanks to I. Haeck for toiling with the manuscript. My research is supported in part by the National Astronomy and Ionosphere Center, which operates the Arecibo Observatory under contract with the NSF.

REFERENCES

Arons, J.: 1979, Space Sci. Rev., 24, 437.
Arons, J.: 1981, these proceedings.
Arons, J. and Scharlemann, E. T.: 1979, Astrophys. J., 231, 854.
Backer, D. C.: 1973, Astrophys. J., 182, 245.
Backer, D. C.: 1976, Astrophys. J., 263, 202.
Backer, D. C. and Rankin, J. M.: 1980, Astrophys. J. Suppl., 42, 143.
Backer, D. C., Rankin, J. M. and Campbell, D. B.: 1976, Nature, 263, 202.
Bartel, N.: 1978, Astron. Astrophys., 62, 393.
Bartel, N. and Sieber, W.: 1978, Astron. Astrophys., 70, 307.
Bartel, N., Sieber, W. and Wolszczan: 1980, Astron. Astrophys., in press
and Bartel, N., Kardashev, N., Kuzmin, A., Nikolaev, N., Popov, M., Sieber, W., Smirnova, T., Soglasnov, V. and Wielebinski, R.: 1980, Astron. Astrophys., in press.
Benford, G.: 1977, Monthly Notices Roy. Astron. Soc., 179, 311.
Blandford, R. D. and Scharlemann, E. T.: 1976, Monthly Notices Roy. Astron. Soc., 174, 59.
Boriakoff, V.: 1976, Astrophys. J. Letters, 208, L43.
Boriakoff, V.: 1980, submitted to Astrophys. J. and these proceedings.
Bruk, Y. M., Davies, J. D., Kuzmin, A. D., Lyne, A. G., Malofeev, V. M., Rowson, B., Ustimenko, B. Y. and Shitov, Y. P.: 1978, Soviet Astron., 22, 588.
Cheng, A. and Ruderman, M.: 1977, Astrophys. J., 212, 800.
Cheng, A. and Ruderman, M.: 1979, Astrophys. J., 229, 348.
Cheng, A. and Ruderman, M.: 1980, Astrophys. J., 235, 576.
Cordes, J. M.: 1976a, Astrophys. J., 208, 944.
Cordes, J. M.: 1976b, Astrophys. J., 210, 780.
Cordes, J. M.: 1978, Astrophys. J., 222, 1006.
Cordes, J. M.: 1979a, Australian J. Physics, 32, 9.
Cordes, J. M.: 1979b, Space Sci. Rev., 24, 567.
Cordes, J. M. and Hankins, T. H.: 1977, Astrophys. J., 218, 484.
Cordes, J. M. and Helfand, D. J.: 1980, Astrophys. J., 15 July.
Cordes, J. M. and Greenstein, G.: 1981, Astrophys. J., submitted.
Cordes, J. M., Rankin, J. M. and Backer, D. C.: 1978, Astrophys. J., 223, 961.

Cordes, J. M., Weisberg, J. M. and Hankins, T. H.: 1980, Astrophys. J., submitted.
Craft, H. D.: 1970, Ph.D. Thesis, Cornell University.
Ferguson, D. C.: 1976, Astrophys. J., 209, 606.
Ferguson, D. C.: 1981, these proceedings.
Ferguson, D. C. and Seiradakis, J.: 1978, Astron. Astrophys., 64, 27.
Ferguson, D. C. and Boriakoff, V.: 1980, Bull. Am. Astron. Soc., 11, 704.
Goldreich, P. and Julian, W.: 1969, Astrophys. J., 157, 869.
Gunn, J. and Ostriker, J.: 1970, Astrophys. J., 160, 979.
Hankins, T. H.: 1971, Astrophys. J., 169, 487.
Hankins, T. H.: 1972, Astrophys. J. Letters, 177, L11.
Hankins, T. H. and Rickett, B. J.: 1975, Methods in Computational Physics, 14, 55.
Hankins, T. H. and Boriakoff, V.: 1978, Nature, 276, 45.
Hankins, T. H. and Cordes, J. M.: 1980, submitted to Astrophys. J. and these proceedings.
Harding, A. and Tademaru, E.: 1981, Astrophys. J., Jan. 15.
Helfand, D. J., Taylor, J. H., Backus, P. R. and Cordes, J. M.: 1980, Astrophys. J., 237, 206.
Huguenin, G. R., Taylor, J. H. and Troland, T. H.: 1970a, Astrophys. J., 162, 727.
Huguenin, G. R., Manchester, R. N. and Taylor, J. H.: 1970b, Astrophys. J., 169, 97.
Jones, P. B.: 1979, Astrophys. J., preprint.
Kennel, C., Fujimura, S. and Pellat, R.: 1979, Space Sci. Rev., 24, 407.
Komesaroff, M.: 1970, Nature, 225, 612.
Manchester, R. N.: 1974, Science, 186, 66.
Manchester, R. N. and Lyne, A. G.: 1977, Monthly Notices Roy. Astron. Soc., 181, 761.
Manchester, R. N. and Taylor, J. H.: 1977, *Pulsars*, Freeman, San Francisco.
Manchester, R. N., Taylor, J. H. and Huguenin, G. R.: 1975, Astrophys. J., 196, 83.
Matese, J. J. and Whitmire, D. P.: 1980, Astrophys. J., 235, 587.
Melrose, D. B.: 1979, Australian J. Phys., 32, 61.
Michel, F. C.: 1969, Astrophys. J., 158, 727.
Michel, F. C.: 1979, Astrophys. J., 227, 579.
Proszynski, M.: 1979, Astron. Astrophys., 79, 8.
Rickett, B. J.: 1975, Astrophys. J., 197, 185.
Rickett, B. J. and Cordes, J. M.: 1981, these proceedings.
Rickett, B. J., Hankins, T. H. and Cordes, J. M.: 1975, Astrophys. J., 201, 425.
Ritchings, R. T.: 1976, Monthly Notices Roy. Astron. Soc., 176, 249.
Ruderman, M.: 1980, in Proceedings of the Ninth Texas Symposium on Relativistic Astrophysics, Ann. N.Y. Acad. Sci., Vol. 336.
Ruderman, M. and Sutherland, P.: 1975, Astrophys. J., 196, 51.
Sieber, W.: 1973, Astron. Astrophys., 28, 237.
Sieber, W., Reinecke, R. and Wielebinski, R.: 1975, Astron. Astrophys., 38, 169.
Stinebring, D. and Cordes, J. M.: 1981, these proceedings.

Sturrock, P.: 1971, Astrophys. J., 164, 529.
Taylor, J. H., Manchester, R. N. and Huguenin, G. R.: 1975, Astrophys. J., 195, 513.
Unwin, S., Readhead, A., Wilkinson, P. N. and Ewing, M.: 1978, Monthly Notices Roy. Astron. Soc., 182, 711.

DISCUSSION

FERGUSON: Doesn't the evidence for polarization changes at the edges of micropulses and within micropulses argue for a geometrical beaming origin of microstructure rather than a temporal modulation?

CORDES: No. Such polarization changes are apparently due to transitions between orthogonal modes, similar to those observed on subpulse timescales. I would attribute these to radiative transfer effects.

KIRK: If radio emission is produced by charged slabs emitting at the local plasma frequency, how is the broadband structure of the micropulses explained?

CORDES: The radiated frequency sweeps from high to low as the slab propagates outward. Hence a broadband micropulse is produced. The time difference between the emission at two frequencies ν_1 and ν_2 is extremely small, namely about $\delta t = \Delta r/\gamma^2 c$. Here $\Delta r = r(\nu_1) - r(\nu_2)$ and γ is the Lorentz factor of the slab. For $\Delta r < r_{Lc}$ and $\gamma = 10^3$, $\delta t \lesssim 0.1$ μs.

https://doi.org/10.1017/S0074180900092767 Published online by Cambridge University Press